

Preliminary Evaluation of Simultaneous Data and Power Transmission in the Same Frequency Channel

Keita Yamazaki*, Yusuke Sugiyama*, Yoshihiro Kawahara[†], Shunsuke Saruwatari* and Takashi Watanabe[‡]

*Shizuoka University, [†]The University of Tokyo, [‡]Osaka University

* Email: {yamazaki, sugiyama}@aurum.cs.inf.shizuoka.ac.jp, saru@inf.shizuoka.ac.jp

[†]Email: kawahara@akg.t.u-tokyo.ac.jp [‡]Email: watanabe@ist.osaka-u.ac.jp

Abstract—Combining wireless transmission of data and power signals enables us to use wireless devices without charging batteries. To improve the utilization of wireless resources, a sender could simultaneously transmit data and power signals in the same frequency channel. A disadvantage of simultaneous transmission is that it induces interference between data and power signals. To minimize the effect of interference, we propose a new frequency-sharing system. The proposed system makes two contributions. The first contribution is interference cancellation of the power signal to receive data from the collided signal using a combination of digital and analog interference cancellation techniques. The second contribution is a media access control protocol to receive the transmitted power effectively by varying the sleep time. To evaluate the performance of the proposed system, we built an experimental apparatus using software-defined radio. Evaluations show that it is feasible to transmit data and power simultaneously using the proposed system.

I. INTRODUCTION

In our daily lives, we use various types of devices that are connected to wireless networks and exchange information with one another. The devices include mobile phones, car navigation systems, heart-rate monitors, and tooth brushes [1]. Such wireless devices are driven by either charged batteries or other external sources. Wireless power transmission [2] enables wireless devices to be powered permanently without the need for changing and charging batteries; this will lead to the invention of new types of wireless devices.

In this study, we use radio waves as the transmission medium as they offer two advantages: (i) long transmission distance and (ii) little calibration effort. In recent years, the depletion of radio resources has become a significant problem owing to the increase in the types of wireless devices. Therefore, wireless power transmission using radio waves needs to be carried out without the depletion of radio resources.

The purpose of our study is to realize simultaneous data and power transmission in the same frequency channel using wireless power transmission and interference cancellation techniques [3], [4]. Figure 1 shows the final goal of our study. The access points cooperatively transmit data and power to wireless sensor nodes over a wireless network. The wireless sensor nodes send back a data signal using the received and charged power. Multiple access points and sensor nodes transmit data bidirectionally, while the access points transmit power to the sensor nodes unidirectionally.

In this paper, we propose a frequency-sharing system for simultaneous data and power transmission in the same frequency channel. We assume that an access point and a

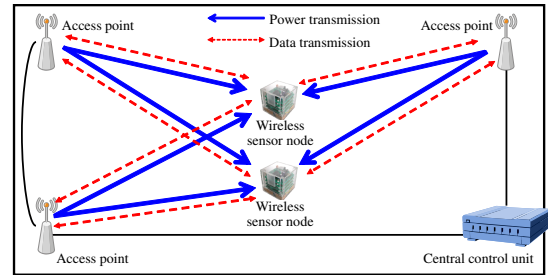


Fig. 1. Final goal of the proposed system.

sensor node transmit data to each other when the access point provides the power to the sensor node. This paper makes two contributions: power-signal interference cancellation and medium access control. Power-signal interference cancellation enables the access point to receive data from a sensor node effectively using digital and analog interference cancellation while transmitting power. Medium access control enables the sensor node to receive the transmitted power effectively by varying the sleep time.

We implemented the proposed system using software-defined radio to evaluate the performance of wireless power transmission and power-signal interference cancellation. We used a WARPv3 software-defined radio [5] to evaluate the feasibility of power transmission. The evaluations show that a sensor node receives power to transmit a packet every 10 seconds.

We also used a universal software radio peripheral (USRP) N200 software-defined radio [6] to evaluate power-signal interference cancellation. Evaluation results show that the digital and analog interference cancellation techniques cancel the power signal by a maximum of 20 dBm and 40 dBm, respectively.

The remainder of this paper is organized as follows. In the next section, we present a brief review of related studies and the position of this study. Section III describes the details of the proposed system that includes a wireless device and a protocol. Section IV evaluates the power transmission and interference cancellation performance of the proposed system. Finally, conclusions are summarized in Section V.

II. RELATED WORK

This study aims to realize simultaneous wireless data and power transmission in the same frequency channel. This simul-

taneous transmission enables us to create a wireless harness or an access point providing data and power simultaneously in vehicles. To achieve simultaneous transmission, the harness or the access point need to cancel interference caused by power signals.

This study focuses on wireless power transmission and interference cancellation. Wireless power transmission is classified into two types: magnetic and radio waves. One of the magnetic products used for wireless power transmission is Felica [7] developed by Sony. Felica transmits power by electromagnetic induction to devices in a few millimeters range.

To increase the distance over which power can be transmitted, several studies have focused on the phenomenon of magnetic resonance. Kurs et al. [8] proposed magnetic resonance-based wireless power transmission. This method utilizes strongly coupled resonance of coils and capacitors and transmits power to devices placed up to a one-meter range. Achieving resonance needs fine-tuning of the coil and capacitor.

A well-known example of wireless power transmission using radio waves is the radio-frequency identifier (RFID) used in various fields. Although the power transmitted by radio waves is less than that by magnetic methods, the radio waves transmit power over longer distances. Yeager et al. [9] demonstrated that power can be received at a distance of 2 m using the UHF band by employing the wireless identification and sensing platform (WISP) [10].

Some studies on energy harvesting have showed that power can be obtained from radio waves in the environment. Kawahara et al. [11] successfully turned on an LED by radio waves from Tokyo Tower and operated a thermometer by utilizing power leakage from a microwave oven. Radio waves are preferred as a medium for wireless power transmission because of the long transmission distance achieved and the little adjustment of devices required.

As regards interference cancellation, some studies have improved communication performance by utilizing the characteristic of simultaneous transmission. A study on successive interference cancellation (SIC) [3], [4], [12], [13], which extracts two data signals from a collided signal, utilizes the difference between the received power of the two signals. In SIC, a collided signal is first decoded to extract a strong data signal while a weak data signal is regarded as interference. The decoded strong signal is then reproduced and the strong signal is subtracted from the collided signal to extract the weaker signal. Finally, the extracted weaker signal is decoded. SIC is performed on the digital signal after auto-gain control (AGC) and analog-to-digital conversion (ADC). SIC is also referred to as digital interference cancellation.

Wireless full duplex communication [14]–[16], which regards its own transmitted signal as self-interference to achieve bidirectional communication, utilizes digital and analog interference cancellation. To cancel self-interference, Bharadia et al. [16] implemented digital and analog interference cancellation on a specific transceiver and achieved high interference cancellation up to a maximum of 110 dB.

Conventional interference cancellation studies focus only

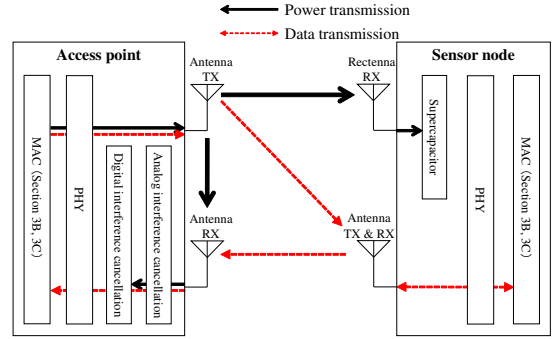


Fig. 2. Overview of the proposed system.

on data transmission. Our study, on the other hand, considers simultaneous data and power transmission using interference cancellation.

III. FREQUENCY-SHARING SYSTEM

Based on the discussion in Section II, we propose a frequency-sharing system for simultaneous data and power transmission. Section III-A describes the architecture of the access point and the sensor node in the proposed system. Section III-B and III-C describe a MAC protocol for uplink and downlink, respectively.

A. The Architecture of the Proposed System

Figure 2 shows the overview of the proposed system. The access point involves digital and analog interference cancellation, the PHY layer, and the MAC protocol described in Section III-B and III-C. The access point has TX and RX antennas. The TX antenna transmits data or power signals from the PHY and the MAC layer.

The TX antenna transmits the power signal continuously unless the access point transmits a data signal. The RX antenna receives the data signal, which is transmitted by a sensor node, and its own power signal. The digital and analog interference cancellation stage extracts the data signal from the received signal. The data signal is processed by the PHY and the MAC layers.

The sensor node has a supercapacitor to store received power. The sensor node also has a MAC protocol described in Section III-B and III-C. The access point has an RX rectenna for power transmission and the TX and RX antennas for data transmission. The RX rectenna receives the power signal and stores the received power in the supercapacitor. The TX antenna transmits the data signal from the PHY layer and the MAC protocol. The RX antenna receives a transmitted data signal from the access point and transfer to the PHY and the MAC layer.

B. Frequency-Sharing MAC Protocol: Uplink

Figure 3 shows the data transmission procedure for uplink. The access point is in the listen state until it receives the data signal. In the listen state, the TX antenna transmits a power signal, and the digital and analog interference cancellation

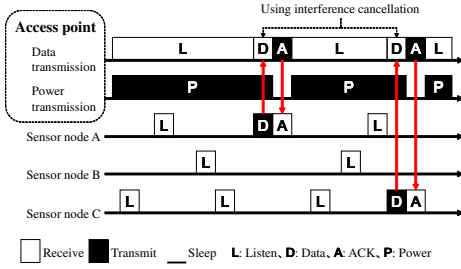


Fig. 3. Data transmission procedure in uplink

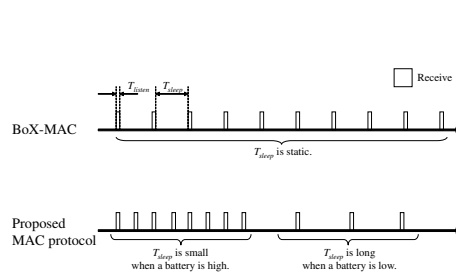


Fig. 4. Comparison of the listen state between BoX-MAC and our proposed system

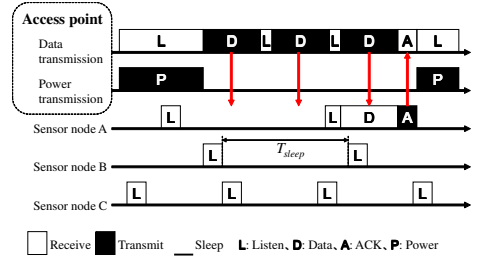


Fig. 5. Data transmission procedure in downlink

stage extracts the data signal from the signal received by the RX antenna.

Each sensor node transmits a data signal without carrier sense when data is generated. After receiving a data signal from a sensor node, the access point stops power transmission and transmits an ACK frame. After transmitting the ACK frame, the access point resumes power transmission. When the sensor node cannot receive the ACK frame, the sensor node retransmits the data signal.

C. Frequency-Sharing MAC Protocol: Downlink

To receive power from an access point efficiently, each sensor node changes its sleep time. To ensure this, we extend the listen state of BoX-MAC [17], which has already been implemented on a CC2420 IEEE 802.15.4 radio transceiver.

Figure 4 shows the comparison of the listen state of the sensor node with that of BoX-MAC. T_{sleep} in BoX-MAC is constant.

On the other hand, our protocol assigns a short T_{sleep} for the sensor node with high battery and a long T_{sleep} for the sensor node with low battery. The protocol calculates T_{sleep} as follows:

$$T_{sleep} = \alpha E_{max} / E_{stored} \quad (1)$$

where α is a weighting factor depending on the application, E_{stored} is the stored power in a sensor node, and E_{max} is the maximum power capacity of the sensor node. When α is large, the average sleep time becomes longer.

Figure 5 shows the data transmission procedure for downlink. The data reception process of each sensor node is the same as that of BoX-MAC. First, each sensor node goes to the listen state during T_{listen} at fixed intervals.

When data is generated at an access point, the access point starts data transmission. The access point repeats data transmission until the access point receives an ACK frame. We assume that sensor node A successfully receives data from the access point for the third time and sends back an ACK frame. Once a sensor node receives data during the listen state, the sensor node stays at the receiving state. After the data is received, the sensor node sends back an ACK frame.

IV. EVALUATION

We evaluated the performance of the system with respect to power transmission and interference cancellation using

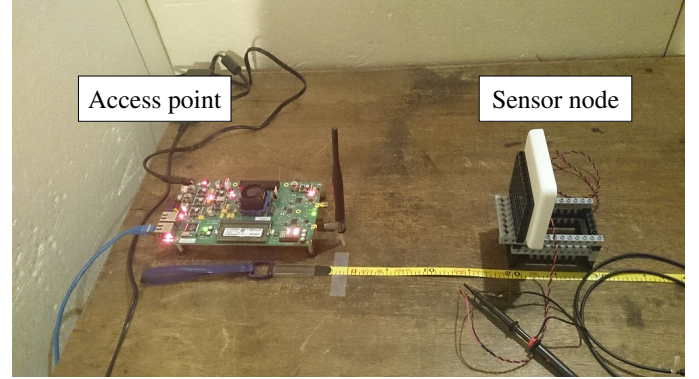


Fig. 6. Power transmission setup

software-defined radio in a preliminary evaluation of the system.

We first implemented power transmission on a WARPv3 software defined radio. The transmission power is 20 dBm, which is the standard transmission power of wireless LANs in Japan. We next implemented interference cancellation on a USRP N200 software-defined radio and a XCVR 2450 with a USRP hardware driver (UHD) [18] using C++. This is because the software-defined radio easily implements digital interference cancellation and adjusts the parameters of analog interference cancellation.

A. Power Transmission

We measured the power received by a sensor node from an access point at the anechoic chamber in Shizuoka University, Japan. Figure 6 shows the power transmission set up. We used a WARPv3 software-defined radio as the access point. The antenna of the access point is VERT2450 for the 2.4–2.48-GHz band with a 3-dBi gain. We connected the WARPv3 software-defined radio to a spectrum analyzer and observed that the transmission power is 17.3 dBm. Thus, the transmission power of the access point with VERT2450 is about 20.3 dBm.

The access point sends three types the power signal: continuous-wave (CW), binary phase-shift keying (BPSK), and orthogonal frequency-division multiplexing (OFDM). We used a rectenna for the 2.4-GHz band as a sensor node and evaluated received power. The received band is $2.45 \text{ GHz} \pm 50 \text{ MHz}$, and the maximum output voltage is $2.7 \text{ V} \pm 0.1 \text{ V}$. We connected the rectenna to a 100-k Ω resistor.

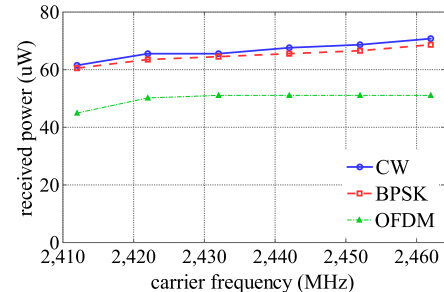
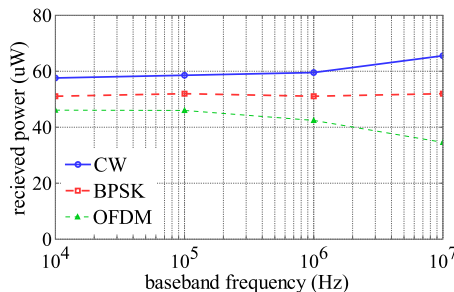
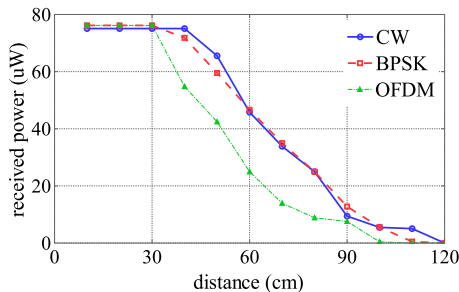


Fig. 7. Received power as a function of the distance

Fig. 8. Received power as a function of the speed of the baseband signal

Fig. 9. Received power as a function of the carrier frequency

Figure 7 shows the received power as a function of distance between the access point and the sensor node. The speed of the baseband signal is 10 Msps. The carrier frequency is 2.412 GHz. Figure 7 shows the following:

- 1) The sensor node receives about $75 \mu\text{W}$ from transmission signals when the distance is shorter than 30 cm.
- 2) The received power of the OFDM signal is lower than that of the CW and the BPSK signals when the access point sends the CW or the BPSK signal when the distance is 30–90 cm. The result shows that a single frequency is more suitable for power transmission than multiple frequencies.
- 3) The received power gradually decreases as the distance increases. The received power is zero when the distance is 120 cm. In order to increase the coverage distance, transmission power has to be increased.

Figure 8 shows the received power as a function of the distance. The carrier frequency is 2.412 GHz. The distance between the access point and the sensor node is 50 cm. Figure 8 shows that the power transmission is almost independent of the speed of the baseband signal. Specifically, the values of received power of the CW, BPSK, and OFDM signals are $57 \mu\text{W}$ – $65 \mu\text{W}$, $51 \mu\text{W}$ – $52 \mu\text{W}$, and $34 \mu\text{W}$ – $46 \mu\text{W}$, respectively.

Figure 9 shows the received power as a function of the carrier frequency. The distance between the access point and the sensor node is 50 cm. The speed of baseband signal is 10 Msps. Figure 9 shows the following:

- 1) Power transmission is almost independent of the carrier frequency. Specifically, the values of received power of the CW, BPSK, and OFDM signals are $61 \mu\text{W}$ – $70 \mu\text{W}$, $60 \mu\text{W}$ – $68 \mu\text{W}$, and $45 \mu\text{W}$ – $51 \mu\text{W}$, respectively.
- 2) The received power of the OFDM signal is 20%–40% lower than that of the CW and BPSK signals. There is room for improvement with respect to the modulation scheme of the data transmission; for example, the modulation schemes on the downlink and uplink can be changed.

The above results show that the sensor node transmits a packet every 10 seconds when the carrier frequency is 2.412 GHz when the distance between the access point and the sensor node is 50 cm, and the speed of the baseband signal is 10 Msps.

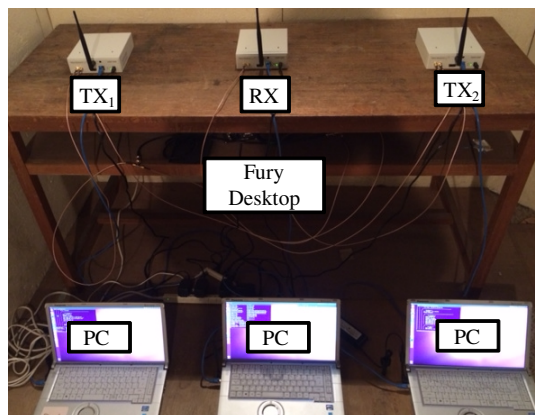


Fig. 10. Experimental setup for digital interference cancellation

This is because the sensor node transmits a packet at $500 \mu\text{J}$. The results demonstrate that the proposed system can be used for short-range wireless applications such as a sensor network in a vehicle.

B. Digital Interference Cancellation

In order to cancel the power signal from the received signal after ADC and AGC, we implemented the digital interference cancellation stage. Figure 10 shows the experimental setup for digital interference cancellation. The experimental setup consists of two senders TX_1 and TX_2 , one receiver RX , three control computers, and a Fury desktop used as an external clock. The senders and the receiver were implemented by USRP N200s and connected to each control PC (Panasonic Let's note CF-B11). To reduce frequency offsets among the USRPs, a 10-MHz signal was input from the Fury desktop to all USRPs. TX_1 periodically sends an OFDM signal as a data signal. TX_2 continuously sends a sine wave as a power signal. The OFDM signal collides with the power signal at RX . RX extracts the OFDM signal by subtracting the power signal from the collided signal. RX decodes the extracted OFDM signal.

We evaluated the experimental setup operating in the 5.11-GHz band at the anechoic chamber in Shizuoka University, Japan. The sampling rate is 195.3125 ksps, and the payload size of the OFDM signal is 1500 bytes. The number of power signal samples was fixed at 500.

First, we evaluated the bit-error rate (BER) as a function of the signal-to noise ratio (SNR). The theoretical values in an

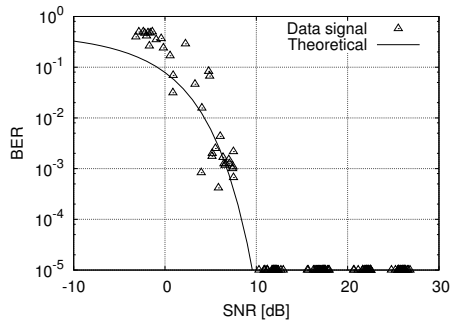


Fig. 11. BER as a function of SNR

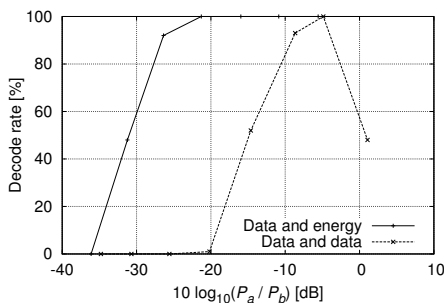


Fig. 12. Decoding rate as a function of power ratio

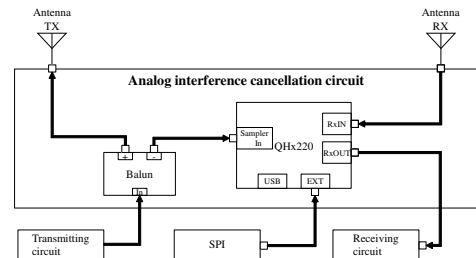


Fig. 13. Schematic of the analog interference cancellation circuit

additive white gaussian noise (AWGN) channel were compared with experimental results. Figure 11 shows the BER as a function of the SNR. The power ratio between the OFDM signal and the power signal ranged from -31.23 to -5.57 dB. If the BER was zero, we plotted for a value of 10^{-5} for convenience sake. Figure 11 shows that digital cancellation is successful because the experimental results approach the theoretical results.

Next, we evaluated the decoding rate as a function of the power ratio. To analyze the difference in performance between cancellation of a known power signal and an unknown data signal, the decoding rates of conventional and our implemented interference cancellation of the power signal were compared.

Figure 12 shows the decoding rate as a function of the power ratio between the two signals. Data and power are proposed for power signal interference cancellation, whereas only data signals are used in conventional SIC. We calculated the power ratio with the received-signal strength indicator (RSSI) of the two signals, P_a and P_b as $10 \log(P_a/P_b)$. In the data and power signal scenario, P_a and P_b are the RSSI of OFDM and power signals, respectively. In the data only scenario, P_a and P_b are the RSSI of weak and strong OFDM signals, respectively. Figure 12 shows the following:

- 1) The decoding rate is small when the power ratio is small. The dynamic range of the data signal becomes smaller because AGC controls the gain based on the power signal. When the power ratio is small, the RSSI of the power signal is larger than that of the data signal. For example, when the power ratio is -30 dB, the RSSI of the power signal is 1000 times larger than that of the data signal.
- 2) The decoding rate of data and power achieved is larger than that achieved with data and data. Unlike the waveform of a power signal, the waveform of a data signal is unknown. When the decoding of a strong data signal fails, the decoding of a weak signal also fails automatically.
- 3) The decoding rate of data and power achieved is 100% when the power ratio is higher than approximately -20 dB. This means that digital interference cancellation is successful when the RSSI of the power signal is about 100 times larger than that of the data signal. When the power ratio is smaller than -20 dB, the receiver needs to combine analog interference cancellation to receive the data signal.

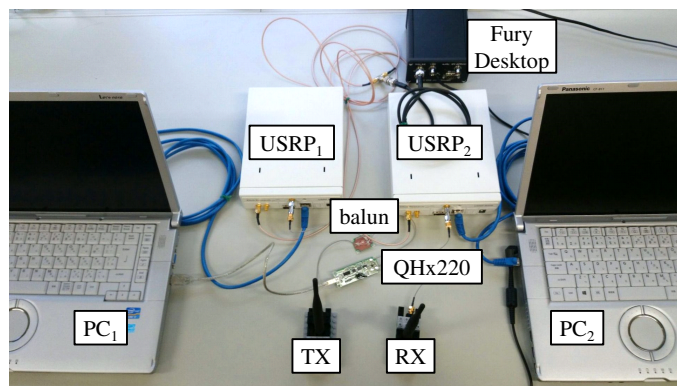


Fig. 14. Experimental setup for analog interference cancellation

C. Analog Interference Cancellation

In order to cancel the power signal from the received signal before AGC and ADC, we implemented the analog interference cancellation circuit using the QHx220 circuit [19]. The QHx220 circuit controls the amplitude and the phase of analog signals. In terms of the number of antennas, the implemented circuit exploits the balun (balanced-unbalanced) circuit to cancel self-interference. Antenna cancellation [15] needs three antennas, whereas the balun circuit needs only two antennas.

Figure 13 shows the schematic of the analog interference cancellation circuit. The transmission signal from a USRP N200 is input to the balun circuit. The balun circuit outputs the phase-inverted transmission signal and the original transmission signal. Next, the phase-inverted transmission signal is input to the QHx220 circuit and the original transmission signal to antenna TX. The QHx220 circuit adjusts the amplitude and the phase of the phase-inverted transmission signal, and the adjusted signal combines with the received signal from antenna RX to achieve self-interference cancellation. The combined signal is fed to another USRP N200, and the amplitude and the phase are adjusted with a serial peripheral interface (SPI) to enhance the performance of interference cancellation. For the adjustment, the SPI uses the result of signal processing and transmits the amplitude and the phase with 24 bits at 10 Mbps.

Figure 14 shows the experimental setup for analog interference cancellation. The experimental setup consists of

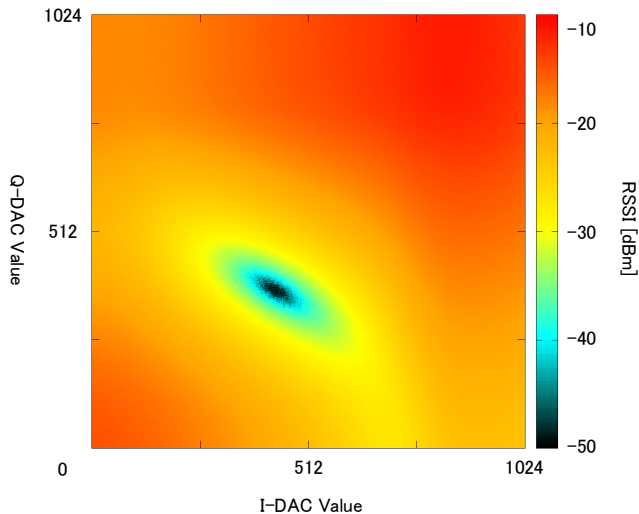


Fig. 15. RSSI of the signal after self-interference cancellation

two USRP N200s, two control PCs (Panasonic Let's note CF-B11), one analog interference cancellation circuit consists of the balun circuit and the QHx220 circuit, and the Fury desktop used as an external clock. To reduce frequency offsets among the USRPs, a 10-MHz signal was input from the Fury desktop to all USRPs. The USRP₁ with the control PC₁ sends the power signal from the antenna TX. After antenna RX received the signal, the analog interference cancellation circuit cancels self-interference. The USRP₂ with the control PC₂ receives the signal. The control PC₂ sends the value of the amplitude and the phase as 78 bytes of data via the USB, whose transmission rate is 921.6 kbps. We used FT245RL to control the QHx220 circuit through the USB. We evaluated the experimental setup operating in the 5.11-GHz band at the anechoic chamber in Shizuoka University, Japan. We observed the RSSI of the signal after self-interference cancellation.

Figure 15 shows the RSSI of the signal after self-interference cancellation. Here, we assign the I-DAC value of the QHx220 circuit parameter to the horizontal axis and the Q-DAC value of the QHx220 circuit parameter to the vertical axis. Figure 15 shows the following:

- 1) The analog interference cancellation circuit cancels self-interference by 40 dB. The circuit achieves better cancellation than digital interference cancellation.
- 2) From the experiment, the optimal I-DAC and Q-DAC values are 377 and 420, respectively. When QHx220 chooses the optimal values, the analog interference cancellation circuits cancels self-interference by 62.4 dB.
- 3) As the I-DAC and Q-DAC values differ from optimal values, the performance of analog interference cancellation gradually decreases. Specifically, the analog interference cancellation circuit cancels self-interference by 40 dB until the I-DAC and Q-DAC values differ from the optimal values by up to 50.

V. CONCLUSIONS

The present paper proposed a frequency-sharing system to transmit data and power wirelessly in the same frequency

channel. To evaluate the performance of power transmission and interference cancellation, we used the software-defined radio. Evaluations showed that the power transmission and the interference cancellation of the wireless device are feasible. Currently, we are working on adapting the system for use in practical applications such as a wireless harness in a vehicle. For future work, we verify our study with theoretical aspects [20], [21].

ACKNOWLEDGEMENT

This work was supported by SCOPE (Strategic Information and Communications R&D Promotion Programme) of Ministry of Internal Affairs and Communications, Japan.

REFERENCES

- [1] Beam, "Beam Toothbrush," <http://www.beamtoothbrush.com/toothbrush/>.
- [2] T. Bieler, M. Perrottet, V. Nguyen, and Y. Perriard, "Contactless power and information transmission," *IEEE Transactions on Industry Applications*, vol. 38, no. 5, pp. 1266–1272, 2002.
- [3] D. Tse and P. Viswanath, *Fundamentals of Wireless Communication*. Cambridge University Press, May 2005.
- [4] D. Halperin, T. Anderson, and D. Wetherall, "Taking the sting out of carrier sense: Interference cancellation for wireless LANs," in *Proceedings of the 14th ACM Annual International Conference on Mobile Computing and Networking (MobiCom'08)*, San Francisco, California, September 2008, pp. 339–350.
- [5] Rice University, "WARP, Rice University open-access research platform," <http://warp.rice.edu/tracl/>.
- [6] Ettus Research, "USRP N200/N210 Networked Series," September 2012.
- [7] Sony Global, "FeliCa Web Site," <http://www.sony.net/Products/felica/>.
- [8] A. Kurs, A. Karalis, R. Moffatt, J. D. Joannopoulos, P. Fisher, and M. Soljacic, "Magnetic resonances wireless power transfer via strongly coupled," *Science*, vol. 317, no. 82, pp. 83–86, July 2007.
- [9] D. J. Yeager, A. P. Sample, and J. R. Smith, "Wisp: A passively powered uhf rfid tag with sensing and computation," *RFID Handbook: Applications, Technology, Security, and Privacy*, pp. 261–278, 2008.
- [10] J. R. Smith, A. P. Sample, P. S. Powladge, S. Roy, and A. Mamishev, "A wirelessly-powered platform for sensing and computation," in *Proceedings of the 8th International Conference on Ubiquitous Computing (UbiComp'06)*, Springer, 2006, pp. 495–506.
- [11] Y. Kawahara, X. Bian, R. Shigeta, R. Vyas, M. M. Tentzeris, and T. Asami, "Power harvesting from microwave oven electromagnetic leakage," in *Proceedings of the 15th International Conference on Ubiquitous Computing (UbiComp'13)*, Zurich, Switzerland, september 2013, pp. 373–382.
- [12] S. Gollakota and D. Katabi, "ZigZag decoding: Combating hidden terminals in wireless networks," in *Proceedings of the Annual Conference of the ACM Special Interest Group on Data Communication (SIGCOMM'08)*, Seattle, Washington, August 2008, pp. 159–170.
- [13] A. Gudipati and S. Katti, "AutoMAC: Rateless wireless concurrent medium access," in *Proceedings of the 18th ACM Annual International Conference on Mobile Computing and Networking (MobiCom'12)*, Istanbul, Turkey, August 2012, pp. 257–268.
- [14] J. I. Choi, M. Jain, K. Srinivasan, P. Levis, and S. Katti, "Achieving single channel, full duplex wireless communication," in *Proceedings of the 16th ACM Annual International Conference on Mobile Computing and Networking (MobiCom'10)*, Chicago, Illinois, September 2010, pp. 1–14.
- [15] M. Jain, J. I. Choi, T. M. Kim, D. Bharadia, S. Seth, K. Srinivasan, P. Levis, S. Katti, and P. Sinha, "Practical, real-time, full duplex wireless," in *Proceedings of the 17th ACM Annual International Conference on Mobile Computing and Networking (MobiCom'11)*, Las Vegas, NV, September 2011, pp. 301–312.
- [16] D. Bharadia, E. McMillin, and S. Katti, "Full duplex radios," in *Proceedings of the Annual Conference of the ACM Special Interest Group on Data Communication (SIGCOMM'13)*, HongKong, China, August 2013, pp. 375–386.
- [17] D. Moss and P. Levis, "BoX-MACs: Exploiting physical and link layer boundaries in low-power networking," Stanford University, Tech. Rep. SING-08-00, 2008.
- [18] J. Blum, "UHD driver for USRPs," in *In GNU Radio Conference (GRC'11)*, September 2011.
- [19] Q. Inc., "QHx220 Active Isolation Enhancer and Interference Canceller," <http://www.intersil.com/products/deviceinfo.asp?pn=QHx220>.
- [20] H. Ju and R. Zhang, "Throughput maximization in wireless powered communication networks," in *IEEE Transactions on Wireless Communications*, vol. 13, no. 1. IEEE, January 2014, pp. 418–428.
- [21] K. Ishibashi, "Dynamic Harvest-and-Forward: New Cooperative Diversity with RF Energy Harvesting," in *Proceedings of the 6th International Conference on Wireless Communications and Signal Processing (WCSP'14)*, October 2014, pp. 1–5.